High-Performance Zeolite T Membrane for Dehydration of Organics by a New Varying Temperature Hot-Dip Coating Method

Xiaoxia Chen, Jinqu Wang, Dehong Yin, Jianhua Yang, Jinming Lu, and Yan Zhang
State Key Laboratory of Fine Chemicals, Institute of Adsorption and Inorganic Membrane, School of Chemical Engineering, Dalian University of Technology, Dalian, Liaoning 116024, China

Zan Chen
Key Laboratory of Catalytic Technology, CNOOC Tianjin Chemical Research & Design Institute, Tianjin 300131, China

DOI 10.1002/aic.13851
Published online June 11, 2012 in Wiley Online Library (wileyonlinelibrary.com).

A new seeding method, namely, varying-temperature hot-dip coating (VTHDC), is proposed for synthesis of zeolite T membranes by secondary hydrothermal growth. The VTHDC method is composed of hot-dip coating at higher temperature, rubbing off the superfluous crystals, and hot-dip coating at lower temperature. It was found that the method was flexible and effective for combined control over the seed suspension concentration, seed size, and coating temperature, leading to combined control of properties of the seed layer over the seed size, thickness, coverage, and defect. A thin continuous, smooth defect-free asymmetric seed layer was achieved consisting of large and small zeolite T seed crystals. The resulting zeolite T membrane M5 exhibited high pervaporation performance with the flux reaching 2.12 and 2.52 kg/m^2 h for the dehydration of 90 wt % EtOH/H_2O and IPA/H_2O mixture, respectively, at 348 K. The corresponding separation factor was up to 1301 and 10,000, respectively. © 2012 American Institute of Chemical Engineers *AIChE J*, 59: 936–947, 2013
Keywords: zeolite T membrane, varying temperature hot dipping coating, pervaporation dehydration, EtOH/H_2O mixture, IPA/H_2O mixture

Introduction

Dehydration of organics for highly purified organic products is essential in the petrochemical, organic chemicals, fine chemicals, pharmaceutical chemicals, and new energy industries. Among them, dehydration of a large varieties of organics aqueous solutions are under acidic conditions, such as purification of ethanol and isopropanol used as solvents in pharmaceutical chemicals and dehydration of ester products. The conventional process for the purification is distillation/rectification or adsorption that is energy intensive. With growing concern for energy conservation and cost expenditure, pervaporation (PV) membrane separation units are emerging as viable options for replacing or supplementing energy-intensive operations, especially for separating azeotrope or close-boiling liquid mixtures.[1,2]

With uniform pores, high separation selectivity, good mechanical strength, chemical resistance, and thermal stability, zeolite membranes have advantages over polymer membranes, especially used in high temperature, high chemically aggressive environment. They have many applications in the fields of molecular separations including gas and liquid and gaseous mixtures,[3–5] membrane reactions,[6] sensors, electrodes,[7] low-*k* dielectric materials,[8] and corrosion protection coating.[9] Among the various types of zeolite membranes,[10–14] zeolite NaA membranes are extremely selective for removal of water from organic solutions by PV or vapor permeation because of their highly hydrophilicity and suitable X-ray diffraction (XRD) pore diameter of 0.41 nm smaller than most organic molecules and larger than water. Mitsui Engineering and Shipbuilding in Japan realized the first large-scale PV plant in 2001 using tubular NaA membranes for dehydration of organic solvents,[15] and intensive efforts are further focused on development of NaA zeolite membrane with more economically feasible fluxes for implementations of NaA zeolite membranes in many fields such as production of bioethanol fuel. Despite the great successful industrial implementations, NaA membranes are not unfortunately competent for dehydration of organic liquids in an acid media, because acid leaches Al from NaA zeolite structure leading to decomposition of NaA zeolite framework thus degradation of separation performance.[16,17]

Generally speaking, with an increase in Al content in the framework, the hydrophilicity of a zeolite membrane increases, whereas the acid resistance simultaneously decreases. Zeolite T with Si/Al ratio of 3–4 is an intergrowth-type zeolite of erionite and offretite that effective pore size for permeation is the pore size of erionite (0.36×0.51 nm^2) because of the stacking faults of erionite sheets in the framework.[18,19] Compared with zeolite NaA membranes and ZSM-5 zeolite membranes, zeolite T membranes with Si/Al ratio of 3–4 are acid-resistant while remaining hydrophilic. Therefore, they have the potential for the PV dehydration organics in an acid media. Report on synthesis of

Correspondence concerning this article should be addressed to J. Yang at yjianhua@dlut.edu.cn.

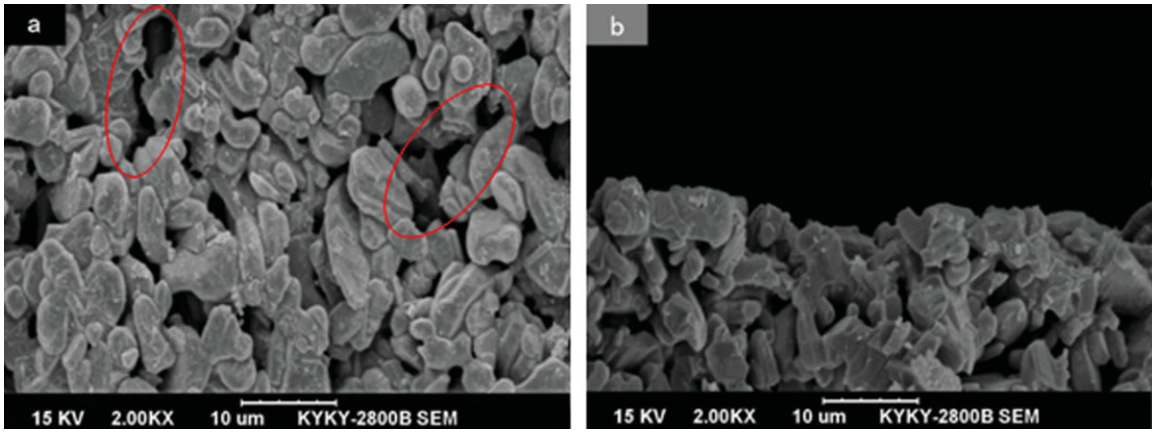

Figure 1. Top and cross-section SEM images of the support (a,b).

[Color figure can be viewed in the online issue, which is available at wileyonlinelibrary.com.]

zeolite T membranes for dehydration of organics was limited. Okamoto and coworkers[20,21] synthesized T zeolite membranes on the mullite tubes by conventional secondary hydrothermal synthesis using rubbing seeding method. The obtained membranes were as thick as 20 μm and showed a total flux of 1.08–1.49 kg/m^2 h with separation of 2200–750 for 10 wt % ethanol aqueous solution at 348 K. Yang and coworkers[22] reported the formation of uniformly a&b-oriented zeolite T membranes using dip-coating by the combined conventional and microwave secondary hydrothermal synthesis. It was found that the orientated seed layer and the combined microwave hydrothermal synthesis were key for obtainment of the orientated zeolite T membrane with high performance.

Secondary growth (seeded growth) is composed of deposition of zeolite seed crystals to form a seed layer[23] and then crystallization of the seeded support to form a polycrystalline zeolite layer. The predeposited zeolite seeds act as nuclei to provide sites for zeolite growth and improve control of crystal growth. The properties of the seed layer including seed size, orientation, coverage, thickness, and defects are, therefore, significant for control of the membrane microstructure such as the thickness, orientation and continuity and the resulting separation performance.[24–26] On the other hand, seeding technique is crucial for manipulating the properties of the seed layer that is influenced by the structures of the substrate as well. Dip-coating,[27] vacuum seeding,[28] rub-coating,[29] and cationic polymer treatment[30] are the most reported seeding methods for preparation of zeolite membranes. By these seeding methods, large efforts are focused on the investigation in effect of either seed size or orientation or the thickness on the separation performance. Combined property control of the seed layer over seed size, coverage, seed layer thickness, and defects for preparation of zeolite membranes is limited. Herein, a combined seed layer manipulation including the seed size, coverage, thickness, and defect and surface roughness by a new varying-temperature hot-dip coating (VTHDC) seeding method is carried out to achieve high-performance zeolite T membrane for dehydration of organics. This method is extension of the dipping–rubbing–dipping seeding method reported in our previous work.[31] The VTHDC method is composed of the following steps: (1) hot-dip coating of seeds using a higher seed suspension at higher temperature; (2) rubbing off the excessive large seeds that loosely attached on the support surface; and (3) hot-dip coating of seeds using a lower seed concentration suspension at lower temperature. By this method, the driving force for deposition of seeds is coaction of the capillary force during the dipping course and the temperature-driven pressure difference caused by the drastical shrink of the air in the confined support due to rapid decrease in temperature. The method is effective and flexible for combined control of surface roughness of support, seed suspension concentration, seed size, and coating temperature. In this way, a thin dense asymmetric T zeolite seed layer with minimizing defects can be obtained. The effects of seed concentration in suspension, the two-step hot coating temperature, crystal size on the properties of seed layer, and the separation performance of the resulting zeolite T membranes were investigated in detail. Comparison of the seed layers and separation performance of the zeolite T membranes by VTHDC method, constant temperature hot-dip coating method (CTHDC), and conventional dip coating (CDC) seeding also carried out. Through the comparison, it is demonstrated that the combined control of seed layer over seed size, coverage, surface roughness, thickness, and defects is crucial for achievement of a high-performance zeolite membrane.

Experimental

Membrane synthesis

Preparation of T Zeolite Seeds and Seed Layers. The zeolite T seeds with different crystal sizes were prepared from a synthesis solution with mole composition of 18.2 SiO_2:Al_2O_3:4.2 Na_2O:1.5 K_2O:0.82 Tetramethyl ammonium hydroxide (TMAOH):212.7 H_2O by controlling the crystallization temperature. The crystallization reaction was carried out at 353 and 373 K for 48 h to obtain zeolite crystal size of 0.4 and 2 μm, respectively. The products were recovered with filtration, washed with deionized water, dried overnight at 333 K, and then calcined in air at 773 K for 6 h. The pure phase of zeolite T crystals was confirmed by XRD patterns. The crystal size was estimated from the SEM observation.

Porous α-Al_2O_3 tubes with mean pore size of 2–3 μm (13-mm outside diameter, 8 mm inside diameter, and 8 cm length, Foshan Ceramics Research Institute (FCRI), China) were used as the supports. Figures 1a, b show the SEM images of the α-Al_2O_3 support. Some large pores up to 20 μm as circle marked can be observed clearly from the top morphology (Figure 1a). The cross-section morphology indicated that the support consisted of disorderly and irregular alumina particles, which resulted in some large caves. The support surface was rather rough and discontinuous, which

Table 1. The Seeding Conditions for the Membranes M1–M7

		Seeding Condition							
		First Step Coating				Second step coating			
Seeding Method	Membr. No.	Seed Concentration (wt %)	Seed Size (μm)	T (K)	Treat Seed Layer	Seed Concentration (wt %)	Seed Size (μm)	T (K)	Treat Seed Layer
OSHDC	M1	3	2	353	No rub	–	–	–	–
	M2	1	2	353	No rub	–	–	–	–
	M3	0.5	2	353	No rub				
	M1′	3	2	448	No rub				
VTHDC	M4	3	2	448	Rub	0.5	2	353	No rub
	M5	3	2	448	Rub	0.5	0.4	353	No rub
CDC	M6	3	2	298	Rub	0.5	0.4	298	No rub
CTHDC	M7	3	2	448	Rub	0.5	0.4	448	No rub

was harmful to prepare a continuous and dense seed layer. The surfaces of the tubes were polished with 800 and 1500 grit-sand paper to smooth the surface. Then, the supports were washed by ultrasonic instrument with acid solution, alkaline solution, and demonized water in turn. Subsequently, the supports were dried overnight in the air oven at 333 K and then calcined in air at 773 K for 6 h for use.

The process of VTHDC seeding is as follows: a specific concentration of seed suspension containing zeolite T crystal and deionized water was prepared with the assistance of ultrasonic at 80 W/h for 40 min to avoid the formation of aggregates. The VTHDC seeding process is composed of three steps. (1) The preheated α-Al_2O_3 tube at 448 K with two ends wrapped with Teflon taps was dipped in the suspension with higher seed concentration for 20 s contact time, then withdrew the tube vertically out of the seed suspension. (2) The precoated support was dried for several hours at room temperature and dried overnight in the air oven at 373 K. Then, the outer surface of the dried support was rubbed using cotton cloth to remove the superfluous and loose T crystals until there were no obvious crystals on the support surface. Again, it was heated at lower temperature of 353 K for next step. (3) The preheated support at 353 K was dipped into the suspension with lower seed concentration for 20 s then withdrew the tube vertically. Below the context, dipping a preheated support at a certain high temperature into the seed suspension solution is called hot-dip coating. In the case that the hot coating temperatures of the steps (1) and (3) are the same, this hot coating process is defined as CTHDC. In the case that only step (1) is carried out, this coating method is defined as one-step hot-dip coating (OSHDC).

For comparison, the supports were seeded by the OSHDC and CTHDC method and the CDC method for preparation of T membranes. The seeding conditions for zeolite T membranes are listed in Table 1.

Preparation of Zeolite T Membrane. The synthesis solution was prepared as follows: the aluminate solution was prepared by dissolving sodium hydroxide (NaOH, Aldrich) and potassium hydroxide (KOH, Aldrich) in deionized water, then adding sodium aluminate ($NaAlO_2$, Aldrich) into the solution. When a clear solution was obtained after about an hour with stirring, the solution was mixed gradually with silica sol (SiO_2 40 wt %, Qingdao Haiyang Chemical). The molar ratio of the resultant synthesis solution was 20 SiO_2:Al_2O_3:5.2 Na_2O:1.8 K_2O:280 H_2O. The resultant solution was stirred for 12 h and a milk-like synthesis gel solution was obtained.

The seeded α-Al_2O_3 tubes were sealed with Teflon caps at both ends and placed vertically in Teflon autoclaves. For all the T membranes, the crystallization reaction temperature and time were kept the same, at 373 K and for 30 h in an air oven. After crystallization, the as-synthesized membranes were removed, washed thoroughly with deionized water, and then dried at 373 K.

Membrane characterization

The morphology and thickness of the as-synthesized T membranes were observed by scanning electron microscopy (SEM) using a KYKY2800B at an acceleration voltage of 15 kV. The crystal structures of the membranes were identified by XRD with a Philips Analytical X-ray diffractometer using Cu Kα radiation.

PV experiments

The properties of the as-synthesized membranes were evaluated by the PV separation of 90 wt % ethanol aqueous solution (EtOH/H_2O) and 90 wt % isopropanol aqueous solution (IPA/H_2O) at 348 K. PV experiments were carried out using an home-made apparatus.[32] The feed solution was stirred vigorously to minimize the effect of concentration polarization. The temperature of the feed was controlled constant by thermocontroller, thermocouple, and heater. The permeate vapor was collected by a cold trap cooled by liquid nitrogen. The downstream pressure was about 80–90 Pa. Composition analysis of the feed and permeate was performed on a gas chromatograph.

The membrane separation performance was evaluated by the permeation flux [Q/(kg/m^2 h)] and the separation factor (S.F.; α). The permeation flux was calculated by the mass of the permeate, which was collected by a liquid-nitrogen trap in a given time interval. The S.F. was determined as

$$\alpha_{A/B} = (Y_A/Y_B)/(X_A/X_B) \quad (1)$$

where X_A and X_B denote the mass fractions of components A and B in the feed, respectively, and Y_A and Y_B the mass fractions of components A and B in the permeate, respectively. A and B represent for water and organic component, respectively.

Results and Discussion

Preparation of the zeolite T membrane by the VTHDC seeding method

Considering that zeolite seeds act as nuclei to provide sites for zeolite growth and improve control of crystal growth, achievement of a seed layer with high coverage, small roughness and controlled thickness, defect-free through a new seeding method is one of key issues for preparation of a zeolite membrane with high performance.

Seed concentration in the coating precursor suspension is one of important factors to control the coverage and thickness of the seed layer. The effect of the seed suspension concentration on the property of the resulting seed layer was examined by OSHDC method and the large T zeolite of 2 μm was used as seeds for the membranes M1–M3 by OSHDC. Figures 2a–f represent the typical SEM images of the seed layer with different seed concentrations suspension. For the high seed concentration of 3 wt %, the support surface of the membrane M1 was fully covered with seeds, but some cracks can be clearly seen in the seed layer. This may attribute to the thick concentration of seed suspension, which made the seed layer too thick. The thickness of the seed layer was about 7 μm. A thick seed layer likely results in the formation of more microcracks during drying and curing because of capillary force stress. These microcracks ultimately affected the quality of membranes. When the seed concentration was 1 wt %, the seed layer for the membrane M2 was smooth with high coverage, but some pinholes were observed. In the case that the seed concentration was further decreased to 0.5 wt %, most of the support surface was covered by the seeds, but still some part of the support surface was naked (Figure 2e). From the cross-section image in Figure 2f, it can be seen that the seed layer was rather thin, even discontinuous. These microcracks or defects or lower coverage ultimately affected the quality of the resulting membranes.

The effect of the hot-dip coating temperature was studied by the OSHDC as well. From the cross-section image of seed layer of the M1 and M1′ obtained at hot-dip coating temperatures of 353 and 448 K, respectively, the seed layer of the membrane M1 seemed more weakly adhensive with the support than the M1′ judging from the observed crevices, as marked with red circle, between seed layer and the support for the M1 but without crevices for M1′. The thickness

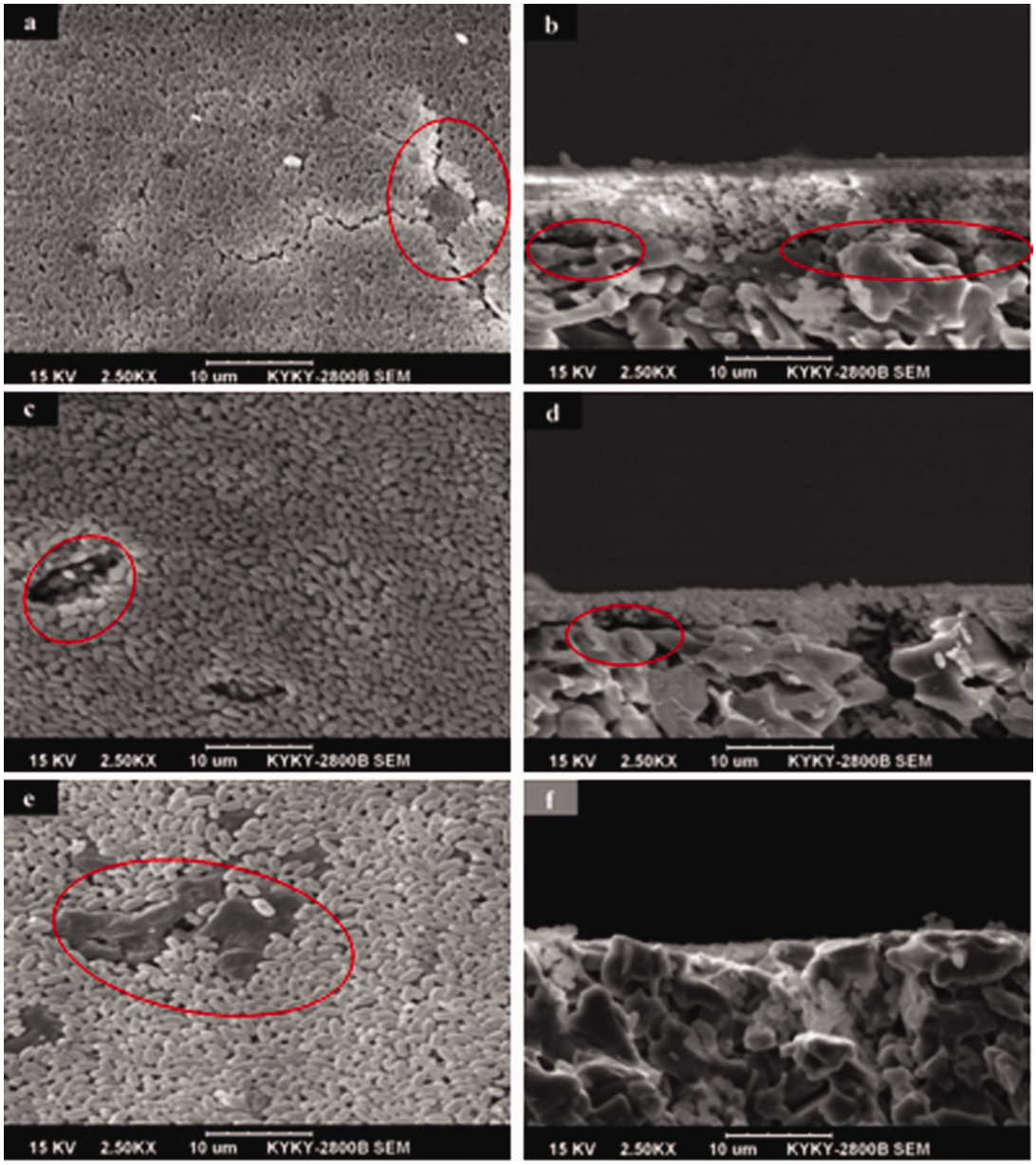

Figure 2. SEM images of the seed layers of the membrane M1 (a,b), M2 (c,d) M3 (e,f), and M1′ (g,h), the seed layer of M4 after rubbing (i_1,j_1), and the seed layer of M4 (i_2,j_2).

[Color figure can be viewed in the online issue, which is available at wileyonlinelibrary.com.]

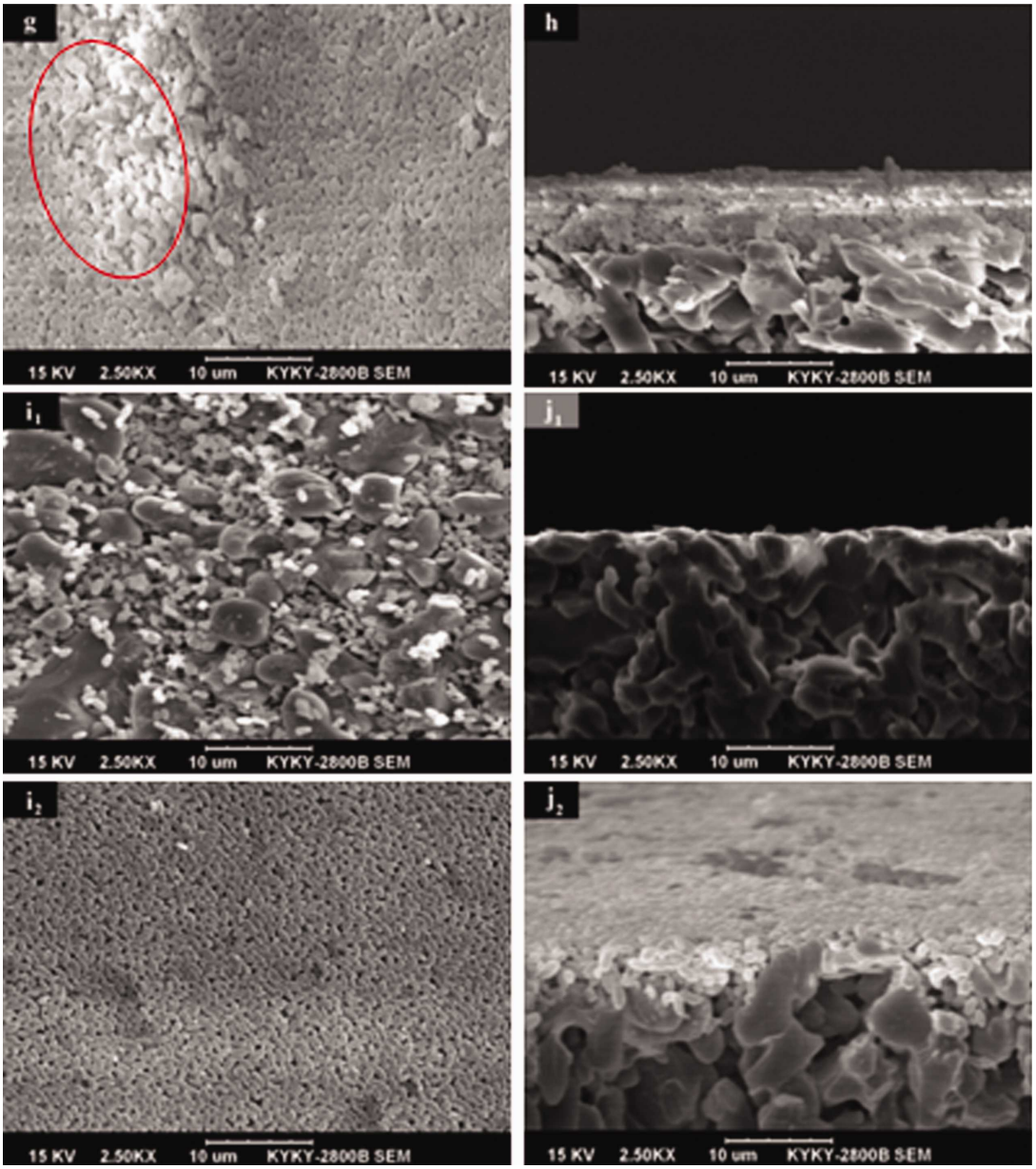

Figure 2. (*Continued*)

was almost the same for the seed layer of the membranes M1 and M1′. However, some islands loosely covered with the seeds were observed on the surface of the seed layer for the membrane M1′ (Figure 2g), which may result from the bubbles generated during dipping course at high temperature over 373 K. As observed above, it is difficult to obtain a thin, dense, continuous, uniform, and defect-free seed layer by OSHDC methods. To overcome this problem, a new seeding method namely the VTHDC was designed. The VTHDC method consists of three steps: (1) hot-dip coating of 3 wt % seed suspension at high temperature of 448 K; (2) rubbing off loose and superfluous seed crystals on the support surface; (3) hot-dip coating of a 0.5 wt % seed suspension at 353 K. Figures $2i_1$, j_1 shows the SEM images of the support of the membrane M4 just after the steps of (1) and (2). At this moment, the large seeds mainly filled into the support pores or voids instead of fully covering the entire surface. And seed islands rather than a continuous and dense seed layer were observed. The large seeds at this stage act as fillers to smooth the support surface and simultaneously reduce pore size of the support to ensure the formation of a continuous, uniform, and dense small seed layer in the next step. The obtained seed layer after step (3) in Figures $2i_2$, j_2 was thin, but dense continuous and uniform without the macrodefect or crack observed. Thickness of the asymmetric seed layer was 2–3 μm much thinner than that of the M1–2.

Pay close attention to the coating steps of the VTHDC, the coating temperature and seed concentration were varied in the first and last step. Besides, rubbing off the seeded support after the first step was carried out. In the first step, the denser seed suspension (3 wt %) was used to seed the support for ensuring a high-coverage seed layer. Meanwhile, the hot-dip coating temperature was increased to 448 K to provide sufficient driving force to make more seeds to penetrate into the large support pores. The precoated support was cured overnight in the air oven at 448 K and rubbed off to remove the loose and redundant crystals on the support surface. It is true that seed islands (Figures $2i_1$, j_1) rather than a dense seed layer was formed after rubbing. Before rubbing,

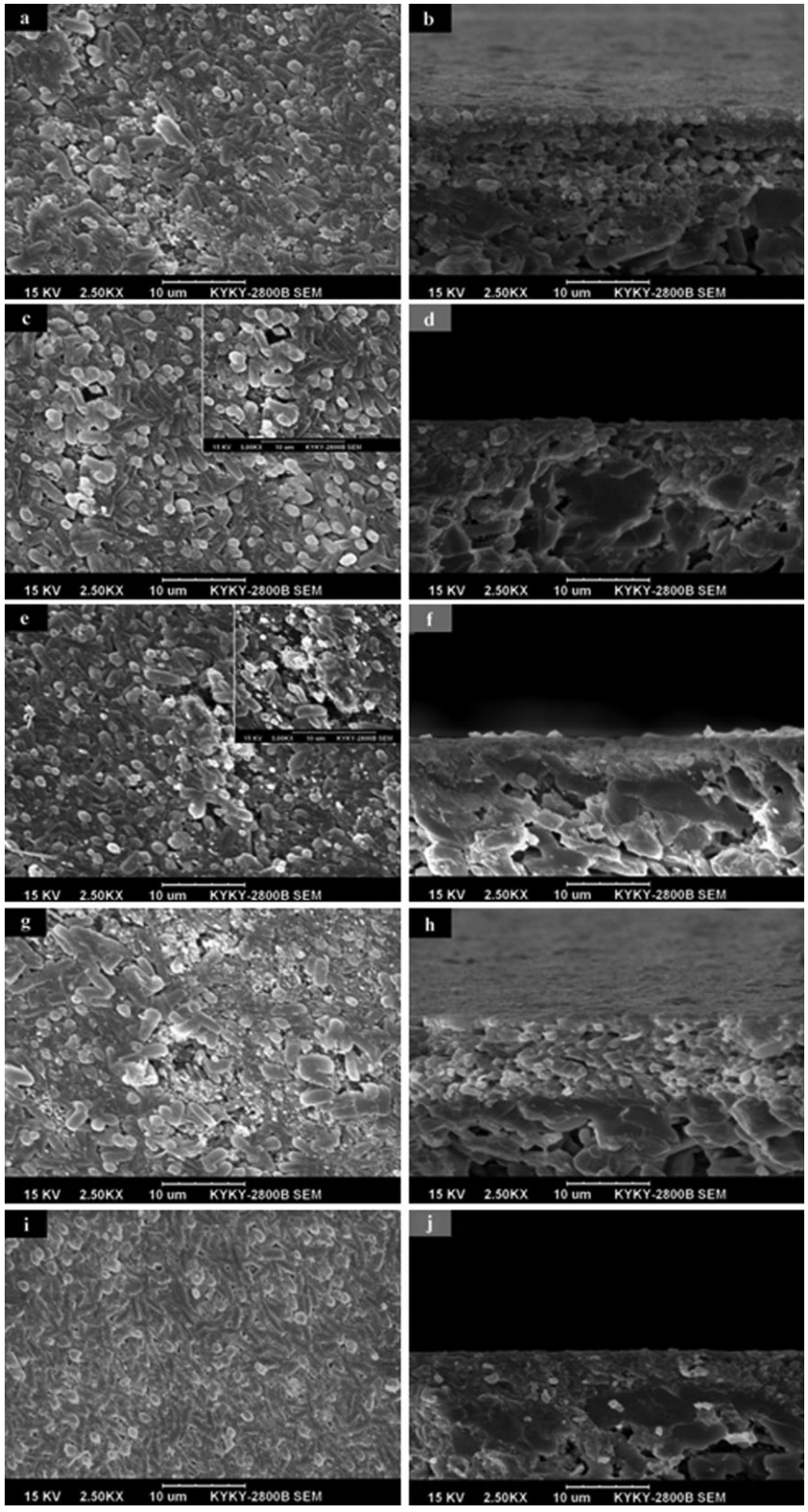

Figure 3. SEM images of the as-synthesized T membrane of M1 (a,b), M2 (c,d), M3 (e,f), M1′ (g,h), and M4 (i,j).

the thickness of the seed layer is as large as 7 μm (Figures 2g, h). The comparison of the seed layer before and after rubbing suggests that the stage of rubbing off plays a very important role in both rubbing off the redundant crystals and cramming some seeds into large pores in the process of the cotton wiping to and from. In the last step, a dilute seed suspension (0.5 wt %) was coated at a relatively lower temperature of 353 K. The varied coating temperature and seed concentration in suspension, as well as rubbing process ensure formation of a thin, continuous, and defect-free seed layer. The detailed principle of the VTHDC will be discussed in the later section again.

Table 2. PV Performances of Zeolite T Membranes by OSHDC and VTHDC Methods for 90 wt % EtOH/H_2O Mixture at 348 K

	PV Performance	
Membrane No.	Flux (kg/m^2 h)	$\alpha_{W/E}$
M1	0.81	96
M2	1.09	165
M3	1.51	306
M1′	1.01	398
M4	1.56	1022

Figures 3a–j show the top and cross-section SEM images of the zeolite T membranes M1–4. The surface of each membrane M1–M1′ is covered by the rice-like zeolite crystals. However, either microcracks or intercrystal voids or large defects as the red circle marked were observed for the four membranes. The microcracks or defects, which are harmful to separation selectivity of the membrane, reasonably resulted from the microcracks or defects or lower seed coverage in the seed layer as stated earlier. The thicknesses of the membranes M1, M1′, M2, and M3 are about 10, 10, 7, and 5–6 μm, respectively, decreasing in sequence of the thickness of the seed layer.

Compared with the membranes M1–M3 and M1′ by OSHDC method, the membrane M4 by the VTHDC method had the better morphology with few defect. The surface of the membrane M4 in Figure 3i was much smoother and denser than those of the membranes M1–M3 and M1′. The cross-section image revealed the membrane M4 (Figure 3j) was dense and continuous, with a thickness of 6–7 μm. It is clear that this continuous and dense morphology of the M4 resulted from the dense, uniform, and defect-free seed layer by the VTHDC.

The PV flux and the separation selectivity for separation of 90 wt % ethanol aqueous solution at 348 K through the membranes M1–4 are given in Table 2. The membrane M4 exhibited the best separation performance with S.F. of 1022 and relatively high flux of 1.56 kg/m^2 h. The membrane M3 showed a similar flux to the M4, but its S.F.. was 306, much lower than the M4. Both the membranes M1 and M2 show poor separation selectivity and flux. The S.F. of the M1′ was higher than that of the M1 with nearly same flux. These obtained separation performance was consistent with the SEM observation as discussed earlier. It is also observed that the flux decreased with the increased membrane thickness. A thin and defect-free T zeolite membrane is desirable for the achievement of high separation performance.

Further optimization of the seed layer through small seeds for achievement of high-performance T zeolite membrane by the VTHDC method

Generally speaking, small seed crystal leads to formation of a thinner and denser membrane with high performance.[28,30,33] Lee et al.[33] reported a thin and high performance silicalite-1 membrane with thickness of 0.3–0.4 μm using sub-40 silicalite-1 crystals. Hedlund et al.[30] fabricated a thin and high-flux silicalite-1 membrane of 0.5 μm using 0.1 μm silicalite-1 crystal seeds. However, in most of cases, a substrate with a small pore size of 0.1–0.2 μm is demanded for seeding such a small seed. Considering the effect of seed size on the grain size, grain shape, and the thickness of the membrane then the resulting membrane separation performance, small zeolite T crystal of 0.4 μm was used as seed as well for preparation of the membrane M5 attempting to obtain higher performance T membrane. The above comparison of the T zeolite membranes by the OSHDC reveals that the VTHDC method is very flexible and effective to control the thickness, coverage, and the defects of the seed layer by controlling the coating temperature, seed concentration. Here, the VTHDC was further demonstrated effective for control the seed size of the seed layer.

Except small zeolite T seeds were used in the third stage, the other seeding conditions and procedures for the membrane M5 were exactly same as the membrane M4 as shown in Table 1. In the third step, instead of the 2-μm zeolite T seeds, the small zeolite T crystals of 0.4 μm were coated onto the support keeping other conditions unchanged. The XRD patterns of the membranes M4 and M5 in Figure 4 represent for the characteristics diffraction peaks of both zeolite T and α-Al_2O_3 support, confirming that the formed membranes M4 and M5 are pure zeolite T phases. Figure 5 gives the SEM image of the obtained seed layer of the M5. It is clearly seen that the seed layer surface coated by small crystals was smooth and dense with few defect compared with the seed layer of the membrane M5 (Figure 2i_2). The seed layer was slightly thinner than that of the M4. The surface of the M5 was covered with a dense layer dotted with warm-like small crystals, very different from the membrane M4. The thickness of the membrane M5 was thinner, about 4–5 μm, than the M4. The different membrane surface morphologies and thicknesses are due to the differences in seed size.

Both the flux and S.F. of the membrane M5 was higher than the membrane M4, reaching 2.12 kg/m^2 h and 1301, respectively (Table 3). This high performance is attributed to the thinner membrane thickness and the dense and compact zeolite T layer with less large defects or grain boudaries that serve as nonselective pathways.

The importance of varying temperature: comparison of the T membranes by the VTHDC and CTHDC and CDC seeding

The Zeolite T Membranes by the CDC and the CTHDC Seeding Method. Figures 6a–d show the seed layers of the membranes M6 and M7 by the CDC and CTHDC methods,

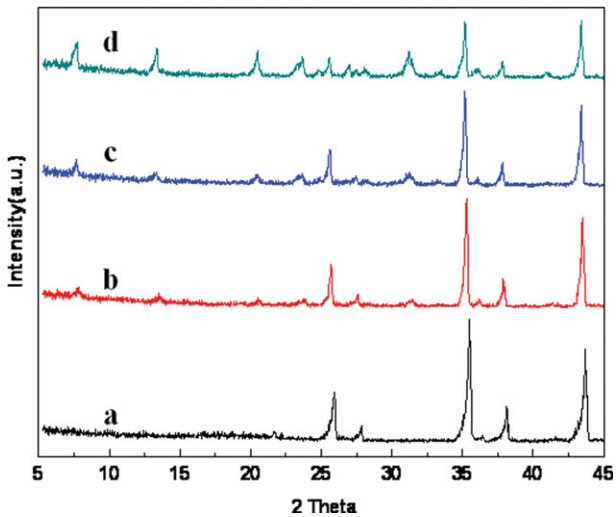

Figure 4. XRD patterns of porous α-Al_2O_3 tube (a), the seeded support (b), the as-synthesized membrane M5 (c), and M4 (d).

[Color figure can be viewed in the online issue, which is available at wileyonlinelibrary.com.]

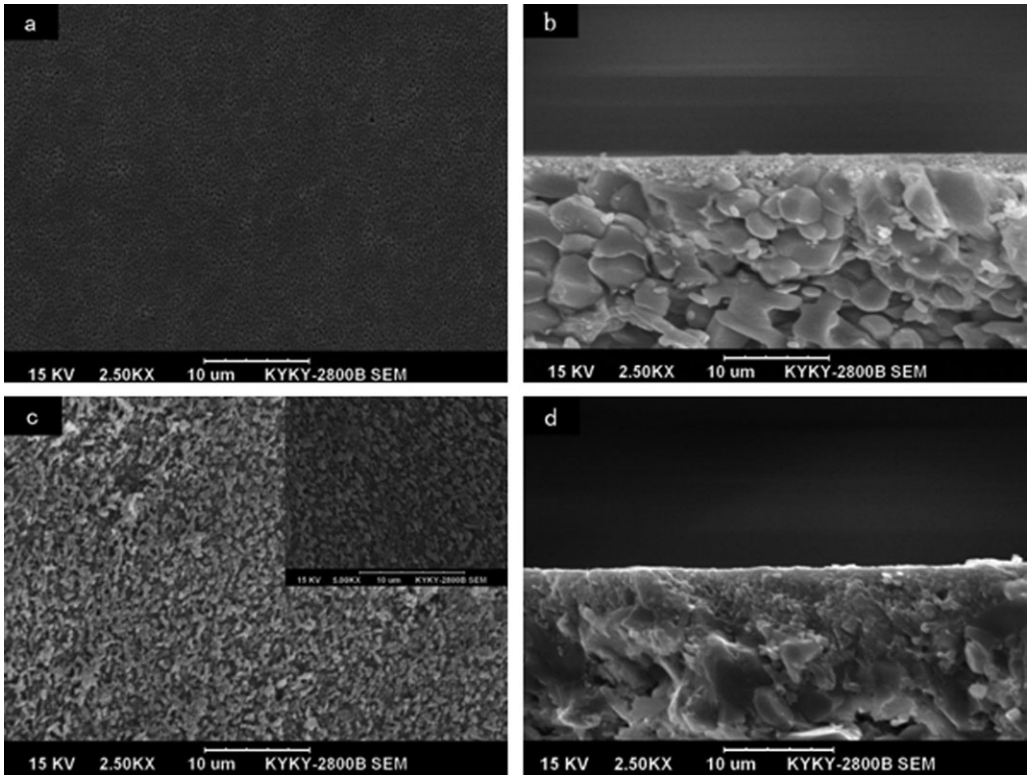

Figure 5. SEM images of the seed layer of membrane M5 (a,b) and the as-synthesized T membrane M5 (c,d).

respectively, using the same seeding conditions except the coating temperature as shown in Table 1. For the membrane M6, the seed layer was not continuous and dense with some alumina particles naked and with some large pinholes observed among the alumina particles. The cross-section image in Figure 6a revealed that some seeds penetrated into the depth of support pores that increased the mass transfer resistance. In contrast, the surface of the seed layer of the M7 (Figure 6c) was much continuous and dense, similar with the seed layer by the VTHDC method, but there was some defect line observed.

Figure 7 shows SEM images of the membranes M6 and M7. Both the surfaces of the membranes M6 and M7 were covered a loose layer with some big defects or visible voids compared with that of the membrane M5. The thickness of each membrane M6 and M7 was similar to the membrane M5, but many small crystals filled into the depth of the support pores in Figure 7b. It is reasonably attributed to the penetration of seeds into the support pores.

PV results were consistent with the SEM image observations. As shown in Table 3, the fluxes of the membrane M6 and M7 were 1.41 and 1.61 kg/m^2, respectively, lower than that of the membrane M5, and the S.F. was only 273 and 329, respectively, much lower than the M5. This lower flux and S.F. were attributed to T zeolite layer deeply penetrated into the support and the big defects existing in the membrane as mentioned earlier.

The membrane M5 by the VTHDC method showed the best separation performance among all the membranes M1–M7 and M1′. The reproducibility is an important criterion for a successful synthesis method. The reproducibility of VTHDC method was investigated and given in Table 4. For the four membranes prepared using the exactly same synthesis conditions by the VTHDC method, three membranes showed almost the same S.F. and permeation flux within about 10% fluctuations, indicating that the VTHDC method has a quite good reproducibility of 75%, similar to that of the OSHDC or CTHDC method (not shown here).

Comparison of Coating Process for the VTHDC, CTHDC, and CDC Method. In this work, the macroporous alumina tube with large average pore size of 2–3 μm and rough surface was used as the support. It is reported that the support accounts for up to 70% of the cost of zeolite membrane. As a result, inexpensive macroporous supports has the potential to reduce the zeolite membrane cost, desirable for industrial application. On the other hand, the larger pore size of the support, the larger the risk of forming defects, which decrease the S.F.. In our work, a thin asymmetric seed layer by VTHDC constituted by large and small seeds was designed to result in a thin and high-performance zeolite T membrane on the macroporous support. The large T seed crystals mainly act as fillers to reduce the roughness and the pore size of the support, whereas small seeds provide high density of nucleation sites to crystal growth and control of membrane microstructure.

The coating process of the VTHDC is illustrated in Figure 8 together with CTHDC and CDC method for comparison. Dip coating is the most used method to deposit sol–gel onto a substrate in the sol–gel processing for the sol–gel film,

Table 3. PV Performances of Zeolite T Membranes by VTHDC, CDC, and CTHDC Methods for 90 wt % EtOH/H_2O Mixture at 348 K

	PV Performance	
Membrane No.	Flux (kg/m^2 h)	$\alpha_{W/E}$
M5	2.12	1301
M6	1.41	273
M7	1.61	329

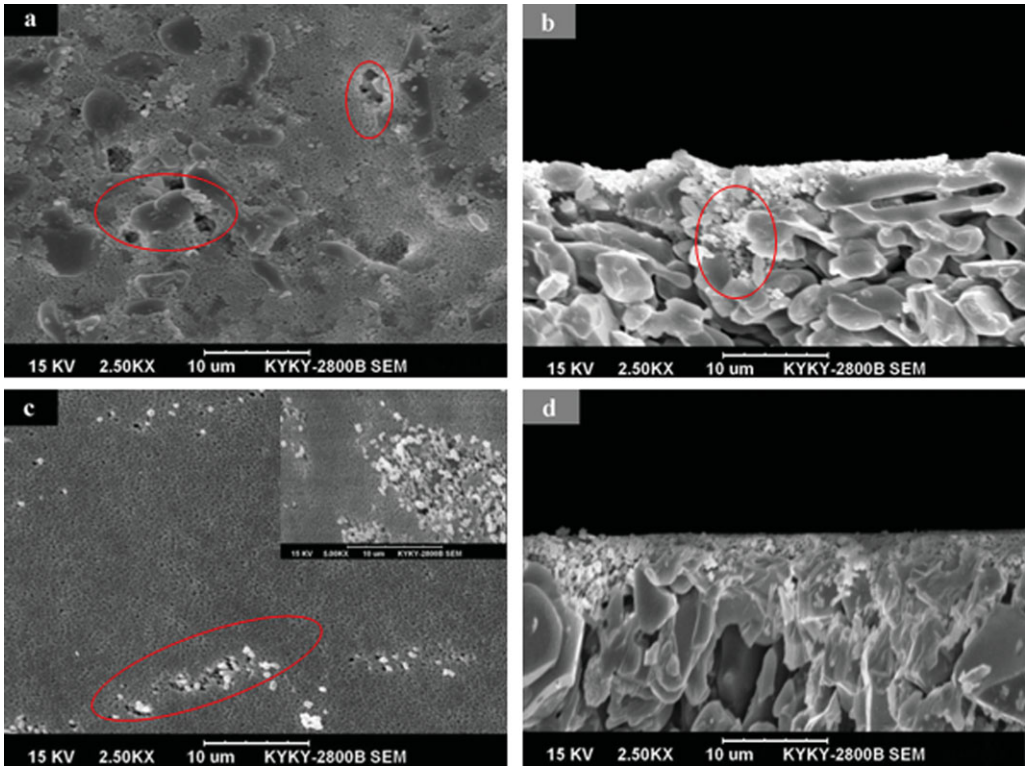

Figure 6. SEM images of the seed layers of membrane M6 obtained by CDC (a,b) and M7 obtained by CTHDC (c,d).

[Color figure can be viewed in the online issue, which is available at wileyonlinelibrary.com.]

sol–gel derived membranes.[34] The driving force of the dip coating is the capillary force. Dip coating was adopted to deposit the zeolite seeds onto the support, namely, CDC seeding during the secondary growth for the zeolite membrane sysnthesis. As well known, the capillary force drives the seed crystals onto the surface of the support during the CDC process, whereas the great gravity of crystals greatly weakens the capillary force. The capilariy force depends on the

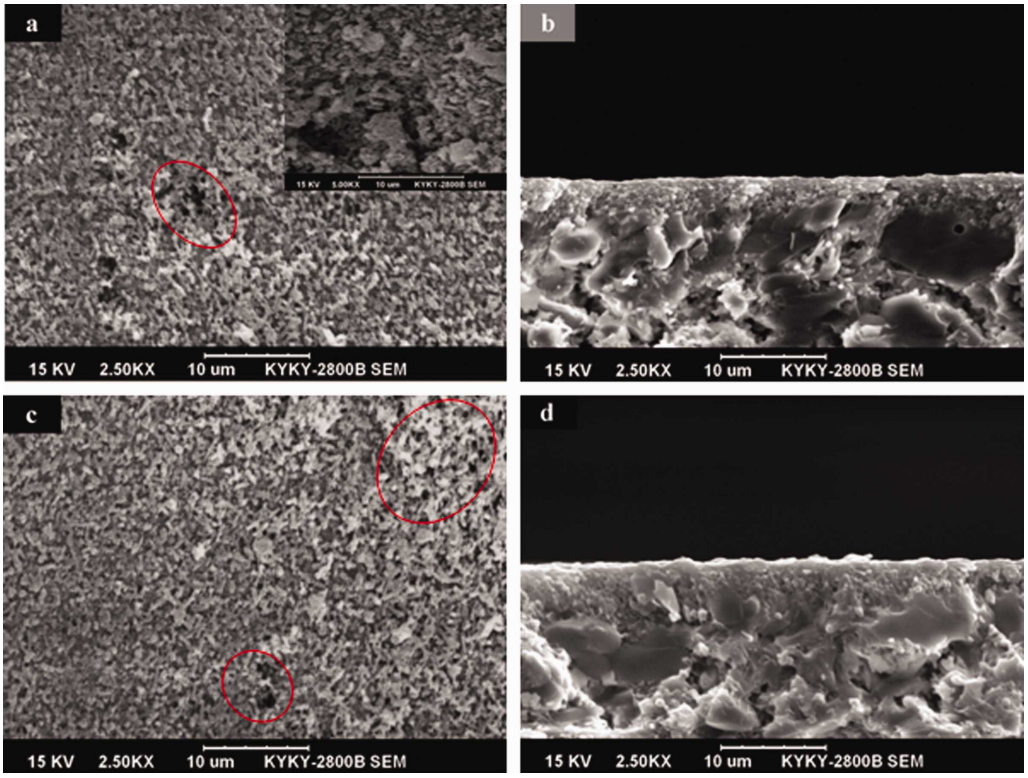

Figure 7. SEM images of the as-synthesized T membrane of M6 (a,b) and M7 (c,d).

[Color figure can be viewed in the online issue, which is available at wileyonlinelibrary.com.]

Table 4. PV Performances of the Zeolite T Membranes Synthesized by VTHDC Method

		PV Performance	
Membrane No.	Seeding Method	Flux (kg/m^2 h)	$\alpha_{W/E}$
M5	VTHDC	2.12	1301
M5-1	VTHDC	1.90	1400
M5-2	VTHDC	2.01	1189
M5-3	VTHDC	1.46	1202

pore size and the liquid/gas/solid interface properties. For the pore diameter of 2–3 μm, the capillary force is as large as 1.46–0.97 bar that should be sufficient to drive the zeolite seeds onto the support surface. On the other hand, some large pinholes or defects inevitably exist in the support as shown in Figure 1a. When the pore diameter is 10 μm, the capillary force is about 0.29 bar. Large zeolite crystals likely cannot be firmly adsorbed onto the support surface of such defects due to larger negative influence of the great gravity and reduced capiliary force. What is more, more seed crystals move to the bottom surface of the support owing to the negative influence of gravitation force, it is also difficult to obtain uniform seeding layer by dip coating method. These are the reasons why the seed layer by the CDC for the membrane M6 is discontinuous and not dense even with the surface of parts of the support naked as shown in Figure 6a.

Hot coating method was first proposed by Asaeda et al.[35,36] to prepare sol–gel derived microporous silica based membranes. Before coating, a substrate was preheated at 180–190°C. Then, a colloidal sol was coated onto the support surface by gently contacting a cloth that was wet with the coating sol. As the substrate is hot enough, the hot coating allows simulaneous coating and gelation to occur instantly on the substrate surface, preventing the sol from penetrating deep into the porous substrate. Also, the hot coating can avoid the capillary force, thus the resulting cracks during the dip coating drying course can be prevented. In such a way, an extremely thin and defect pinholes free silica or silica–ziroconia membranes exhibiting high flux and high selectivity could be obtained.[37–40] In this work, the hot-dip coating was modified to deposit zeolite seeds onto a support surface. A preheated support with two ends sealed was rapidly dipped into the seed suspension solution, namely hot-dip coating seeding. However, the hot-dip coating mechanism for deposition of zeolite seeds is quite different from the hot coating for silica-based sol deposition. The air in the pores and tubular chamber of the hot support will shrink drastically upon rapidly dipping into the seed suspension, resulting in the generation of pressure difference (referred to temperature-driven pressure difference) between the shell and tube sides of the support. Consequently, the hot-dip coating is similar to the vacuum seeding, the zeolite seeds are moved to the support surface under the coaction driving force of the capillary force and temperature-driven pressure difference as shown in Figure 8. The temperature-driven pressure difference depends only on the coating temperature not on the pore size. When the coating temperature is 448 K, the pressure difference is about 0.34 bar determined by the equation of ideal gas state equation. This pressure difference particularly plays a significant role in driving the large zeolite seeds onto the surface of pinholes or large defects larger than 10 μm, because the capillary force decreases with increasing pore size and is about 0.29 bar for pore of 10 μm, smaller than pressure difference. Furthermore, for the most of pore surface of the support, the negative influence of gravitation force during the dip coating course can be offset by the assistance of pressure difference. Therefore, the zeolite seeds can be attracted and transported to over the whole area of the support surface homogenously, likely forming much smoother and much more uniform seeding layer. Obviously, hot coating temperature is vital. When the support temperature is higher than 373 K, the liquid water around the support surface vaporizes, leading to generation of lots of bubbles that are harmful to compactness of the seed layer. It is true that as shown in Figure 6c, for the membrane M7 seeding at 448 K by the CTHDC, most of the surface of the seed layer was continuous and highly dense, but a few parts had some loose particles and holes appeared in the surface. This is due to the bursting of the generated bubbles resulting from the high coating temperature of 448 K.

The VTHDC method can overcome the drawback of the CTHDC method. By the VTHDC method, the coating temperature of the second step is decreased to below 373 K to eliminate the negative influence of bubbles, whereas the first step is maintained at much higher temperature to provide a high driving force to move the large seeds to surface of the support especially to coat the large seeds onto the large defects or pinholes. In the case of the membrane M5, the coating temperatures of the first and second step were set at 448 and 353 K, respectively. The obtained seed layer surface was rather smooth and dense without visible defect existing in the SEM image due to the elimination of the negative influence of the bubbles.

Except control of the coating temperature, the VTHDC method is flexible and effective for combined control over the seed suspension concentration, seed size, leading to combined control of properties of the seed layer over the seed

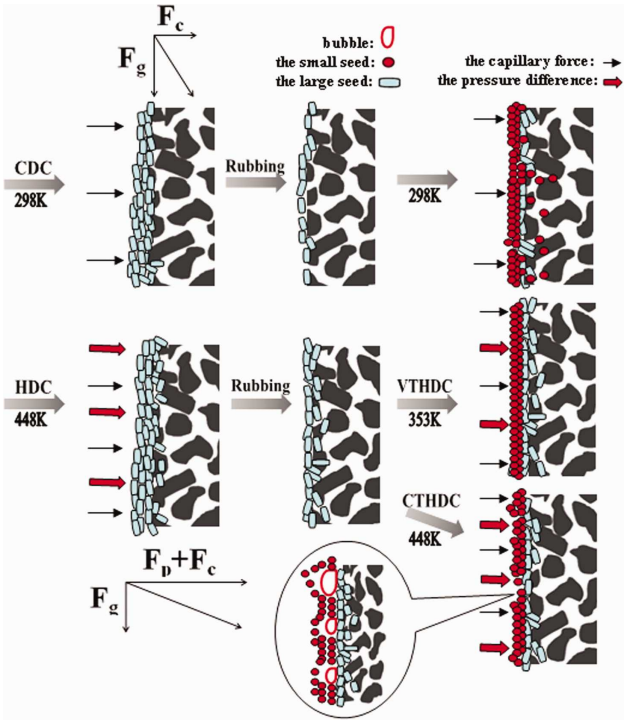

Figure 8. Schematic diagram of coating process of the CDC, CTHDC, and VTHDC method.

[Color figure can be viewed in the online issue, which is available at wileyonlinelibrary.com.]

Table 5. PV Performances of Zeolite T Membranes for Dehydration 90 wt % Alcohol/Water Mixtures

Feed mixture (Alcohol Content 90 wt %)	Temperature (K)	Flux (kg/m^2 h)	$\alpha_{W/E}$	Ref.
EtOH/H_2O	348	2.12	1301	This work
IPA/H_2O	348	2.52	10,000	
EtOH/H_2O	338	1.77	1116	22
IPA/H_2O	338	2.15	10,000	
EtOH/H_2O	348	1.1	900	21
IPA/H_2O	348	2.2	8900	
EtOH/H_2O	348	1.25	2200	41
IPA/H_2O	348	1.77	10,000	

size, thickness, coverage, and defect which is significant for achievement of a high-performance zeolite membrane.

Comparison of the PV performance

The separation performance of the membrane M5 was further examined using 90 wt % IPA/H_2O mixture at 348 K as shown in Table 5. The membrane M5 exhibited a high PV performance with total flux of 2.52 kg/m^2 h and S.F. as high as 10,000. The higher flux and S.F. are due to larger IPA molecule (IPA 0.45 nm, EtOH 0.43 nm) as well as the higher driving force resulting from the higher equilibrium water partial pressure and lower IPA partial pressure in IPA/H_2O mixture than that in EtOH/H_2O mixture.

The PV performances of the membrane M5 are also compared with the reported ones in the literature[21,22,41] as given in Table 5. Considering the temperature effect, the PV performance of the membrane M5 in this work was almost the same as that of the best T membrane reported so far,[22] which was prepared first by conventional secondary hydrothermal growth further by microwave hydrothermal synthesis for repairing the defects. In our work, the membrane M5 was prepared by only a single step hydrothermal synthesis. The high performance of M5 is due to the manipulated thin seed layer with suitable seed size, high coverage, and free defect by the VTHDC method. The work demonstrated that the importance of control of the microstructure of the seed layer and development of seeding technique.

Conclusions

A new VTHDC seeding method based on pressure difference resulting from the rapid temperature drop is developed for synthesis of high-performance zeolite T membranes on coarse macroporous alumina supports. The VTHDC method is composed of hot-dip coating at higher temperature 448K–rubbing–hot-dip coating at lower temperature. This method is found flexible and effective for combined control of the seed suspension concentration, seeding temperature, and seed size. By the method, a combined seed layer manipulation including the seed size, coverage, thickness, and defect and surface roughness can be realized. A thin continuous, smooth defect-free asymmetric seed layer of zeolite T was achieved consisting of large and small seed crystals of 2 and 0.4 μm, respectively. The large seeds mainly act as filler to reduce the pore size and surface roughness of the support, whereas the small seeds serve to provide nucleation sites for the growth of T crystals. The resulting zeolite T membrane M5 showed a total flux of 2.12 kg/m^2 h and S.F. of 1301 for 90 wt % EtOH aqueous solution at 348 K. A better total flux of 2.52 kg/m^2 h and S.F. of 10,000 through the membrane M5 was obtained for the IPA/H_2O at the same PV conditions.

The comparison of separation membranes by the VTHDC, CTHDC, and CDC methods demonstrates that the VTHDC method is effective and flexible for the combined control of seed layer properties over coverage, seed size, thickness, and defect.

Literature Cited

1. Lipnizki F, Field RW, Ten PK. Pervaporation-based hybrid process: a review of process design. *J Membr Sci*. 1999;153:138–210.
2. Feng X, Huang RYM. Liquid separation by membrane pervaporation: a review. *Ind Eng Chem Res*. 1997;36:1048–1066.
3. Coronas J, Santamaria J. Separations using zeolite membranes. *Sep Purif Method*. 1999;28:127–177.
4. Urtiaga A, Gorri ED, Casado C, Ortiz I. Pervaporative dehydration of industrial solvents using a zeolite NaA commercial membrane. *Sep Purif Technol*. 2003;32:207–213.
5. Noack M, Kolsch P, Seefeld V, Toussaint P, Georgi G, Caro J. Influence of the Si/Al-ratio on the permeation properties of MFI-membranes. *Micropor Mesopor Mater*. 2005;79:329–337.
6. Cheng XL, Wang ZB, Yan YS. Corrosion-resistant zeolite coating by in situ crystallization. *Electrochem Solid-State Lett*. 2001;4: B23–B26.
7. Kornic S, Baker M. Nanoporous zeolite film electrodes. *Chem Commun*. 2002;16:1700–1701.
8. Wang Z, Wang H, Mitra A, Huang L, Yan Y. Pure-silica zeolite low-k dielectric thin films. *Adv Mater*. 2001;13:746–749.
9. Lai SM, Ng CP, Martin-Aranda R, Yeung KL. Knoevenagel condensation reaction in zeolite membrane microreactor. *Micropor Mesopor Mater*. 2003;66:239–252.
10. Bein T. Synthesis and applications of molecular sieve layers and membranes. *Chem Mater*. 1996;8:1636–1653.
11. Tavolaro E, Drioli E. Zeolite membranes. *Adv Mater*. 1999;11:975–996.
12. Caro J, Noack M, Kölsch P, Schäfer R. Zeolite membranes—state of their development and perspective. *Micropor Mesopor Mater*. 2000;38:3–24.
13. Lin YS, Kumakiri I, Nair BN, Alsyouri H. Microporous inorganic membranes. *Sep Purif Method*. 2002;31:229–379.
14. Bowen TC, Noble RD, Falconer JL. Fundamentals and applications of pervaporation through zeolite membranes. *J Membr Sci*. 2004; 245:1–33.
15. Morigami Y, Kondo M, .Abe J, Kita H, Okamoto K, The first large-scale pervaporation plant using tubular-type module with zeolite NaA membrane. *Sep Purif Technol*. 2001;25:251–260.
16. Szostak R. *Molecular Sieves, Principles of Synthesis and Identification*. New York: Van Nostrand Reinhold, 1989:313.
17. Muller M, Harvey G, Prins R. Comparison of the dealumination of zeolites beta, mordenite, ZSM-5 and ferrierite by thermal treatment, leaching with oxalic acid and treatment with SiCl4 by 1H, 29Si and 27Al MAS NMR. *Micropor Mesopor Mater*. 2000;34:135–147.
18. Lillerud KP, Raeder JH. On the synthesis of erionite-offretite intergrowth zeolites. *Zeolites*. 1986;6:474–483.
19. Wang X, Xu R. Studies on the transformation between erionite and offretite in T-type zeolite. *Stud Surf Sci Catal*. 1985;24:111–118.
20. Cui Y, Kita H, Okamoto K. Preparation and gas separation performance of zeolite T membrane. *J Mater Chem*. 2004;14:924–932.
21. Cui Y, Kita H, Okamoto K. T Zeolite membrane: preparation, characterization, pervaporation of water/organic liquid mixtures and acid stability. *J Membr Sci*. 2004;236:17–27.
22. Zhou H, Li YS, Zhua GQ, Liu J, Yang WS. Microwave-assisted hydrothermal synthesis of a&b-oriented zeolite T membranes and their pervaporation properties. *Sep Purif Technol*. 2009;65:164–172.
23. Lovallo MC, Tsapatsis M. Preferentially oriented submicron silicalite membranes. *AIChE J*. 1996;42:3020–3029.
24. Shao J, Ge Q, Shan L, Wang Z, Yan Y. Influences of seeds on the properties of zeolite NaA membranes on alumina hollow fibers. *Ind Eng Chem Res*. 2011;50:9718–9726.
25. Lai ZP, Bonilla G, Diaz I, Nery JG, Sujaoti K, Amat MA, Kokkoli E, Terasaki O, Thompson RW, Tsapatsis M, Vlachos DG. Microstructural optimization of a zeolite membrane for organic vapor separation science. *J Sci*. 2003;300:456–460.
26. Choi J, Ghosh S, Lai ZP, Tsapatsis M. Uniformly a-oriented MFI zeolite films by secondary growth. *Angew Chem Int Ed Engl*. 2006;45:1154–1158.

27. Shao GL, Yang JH, Zhang XF, Zhu G, Wang JQ, Liu C. Seeded growth of beta zeolite membranes using zeolite structure-directing agent. *Mater Lett*. 2007;61:1443–1445.
28. Huang AS, Lin YS, Yang WS. Synthesis and properties of A-type zeolite membranes by secondary growth method with vacuum seeding. *J Membr Sci*. 2004;245:41–51.
29. Kusakabe K, Kuroda T, Murata A, Morooka S. Formation of a Y-type zeolite membrane on a porous α-alumina tube for gas separation. *Ind Eng Chem Res*. 1997;36:649–655.
30. Hedlund J, Sterte J, Anthonis M, Bons AJ, Carstensen B, Corcoran N, Cox D, Deckman H, Gijnst WD, Moor PP, Lai F, McHenry J, Mortier W, Reinoso J, Peters J. High-flux MFI membranes. *Micropor Mesopor Mater*. 2002;52:179–189.
31. Xiao W, Chen Z, Zhou L, Yang JH, Lu JM, Wang JQ. A simple seeding method for MFI zeolite membrane synthesis on macroporous support by microwave heating. *Micropor Mesopor Mater*. 2011;142:154–160.
32. Chen Z, Yang JH, Yin DH, Li YH, Wu SF, Lu JM, Wang JQ. Fabrication of poly 1-vinylimidazole/mordenite grafting membrane with high pervaporation performance for the dehydration of acetic acid. *J Membr Sci*. 2010;349:175–182.
33. Lee PS, Zhang XY, Stoeger JA, Malek A, Fan W, Kumar S, Yoo WC, Hashimi SA, Penn RL, Stein A, Tsapatsis M. Sub-40 nm zeolite suspensions via disassembly of three-dimensionally ordered mesoporous-imprinted silicalite-1. *J Am Chem Soc*. 2011;133:493–502.
34. Brinker CJ, Scherer G. *Sol–Gel Science, the Physics and Chemistry of Sol-Gel Processing*. San Diego: Academic Press, 1990.
35. Asaeda M, Kitao S. Separation of molecular mixtures by inorganic porous membranes of ultra fine pores. *Key Eng Mater*. 1991; 61&62:295–300.
36. Asaeda M, Okazaki K, Nakatani A. Preparation of thin porous silica membranes for separation of non-aqueous organic solvent mixtures by pervaporation. *Cream Trans*. 1992;31:411–420.
37. Asaeda M, Yamamichi A, Satoh M, Kamakura M. Preparation of Porous Silica Membranes for separation of propylene/propane mixture. In Y.Y. Ma (Ed.). Massachusetts: Worcester Polytechnic Institute. Proceeding of the Third International Conference on Inorganic Membranes. 1994: 315–323.
38. Asaeda M, Yamasaki S. Separation of inorganic/organic gas mixtures by porous silica membranes. *Sep Purif Technol*. 2001;25:151–159.
39. Tsuru T. Inorganic porous membranes for liquid phase separation. *Sep Purif Methods*. 2001;30(2):191–220.
40. Yang J, Yoshioka T, Tsuru T, Asaeda M. Pervaporation characteristics of aqueous–organic solutions with microporous SiO_2–ZrO_2 membranes: experimental study on separation mechanism. *J Membr Sci*. 2006;284:205–213.
41. Takaki S, Kita H, Okamoto KI, *Symp Ser Soc Chem Eng Jpn*. 1988;66:90–92.

Manuscript received Jan. 25, 2012, revision received Mar. 31, 2012, and final revision received May 17, 2012.